URBAN DEVELOPMENT DIRECTORATE (UDD)

Ministry of Housing and Public Works

Government of the People's Republic of Bangladesh

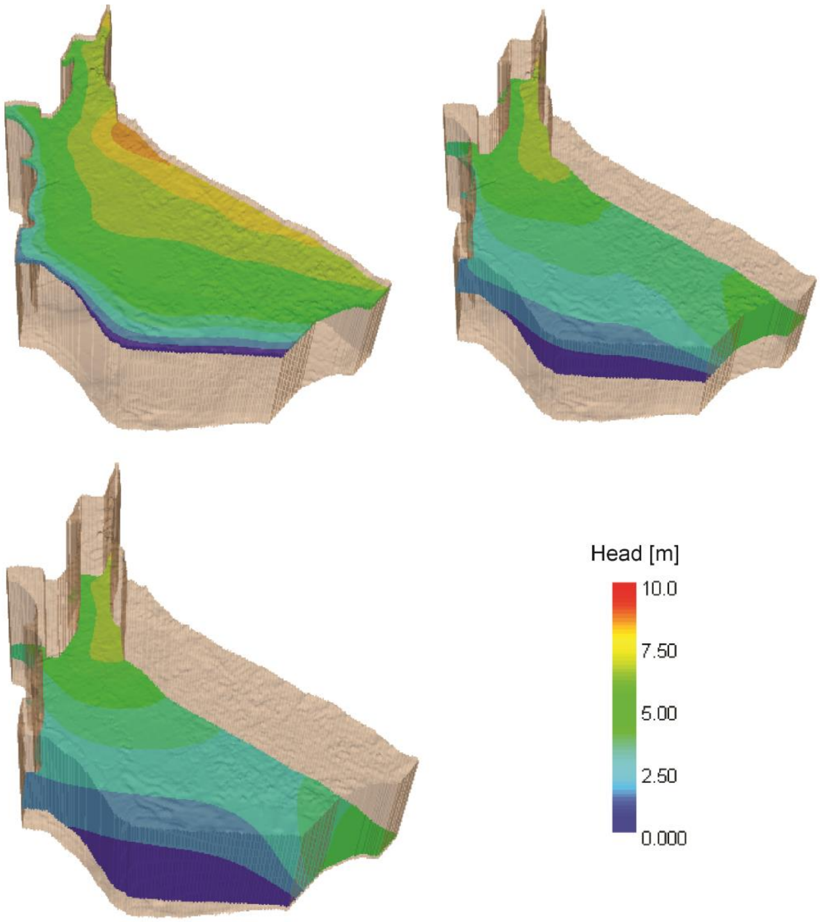

DRAFT FINAL Report
On
HYDRO-GEOLOGICAL
SURVEY UNDER MIRSHARAI
UPAZILA DEVELOPMENT PLAN
(MUDP)

Package No.: 5 (Five)

July, 2018

Submitted by

CENTER FOR GEOSERVICES & RESEARCH

Center for Geoservices and Research

Flat# GCA (Gr. Floor), House # 409, Road # 06, Mirpur DOHS, Dhaka-1216.

Contents

List of Figures

List of Tables

1. Introduction

Water is the most important constituent of life. Every human activity requires water. The Mirashrai Upazila of Chittagong district is likely to experience rapid industrialization and urbanization in the near future as the largest economic zone in Bangladesh is proposed to be developed in this Upazila. Both industrialization and urbanization have large impacts on water as these activities increases demands of water as well as poses threat to water contamination. To characterize the current water situation, to identify suitable locations for water resources development, and to identify risk of water contamination the Urban Development Directorate (UDD) have initiated a hydrogeological investigations throughout the Upazila. 'Center for Geoservices and Research' was employed by UDD to carry out the study in the Upazila.

The aim of hydrology and hydro-geological study for the study areas of Mirshari Region is to identify the surface water body and aquifer of the region including its seasonal variation. The study is also intended to identify the availability fresh ground water, which would be required for the additional people including tourists after implementation of the project, i.e. the foundation of the economic zone. This study comprises of Hydro-geological and geophysical investigations and ground water modeling, water quality mapping, surface water distribution and its management planning by using those data.

1.1. Location and Accessibility

Mirsharai Upazila (Chittagong District) is located between 22˚39′ and 22˚59′ north latitudes and between 91˚27′ and 91˚39′ east longitudes and has an area of 482.88 km^2 (BBS). It is bounded by the Feni River in the North, Sitakunda upazila in the south, Chittagong hill tracts in the east, and the Sandwip Chanel in the west. Mirsharai Thana was founded in 1901 and it was turned into an Uapazila in 1983. Mirsharai Upazila consists of 2 Municipality, 16 Union and 113 Mouza with a total population of 398,716 (Three Lakh Ninety Eighty Thousand Seven Hundred Sixteen).

The Upazila is located at a distance of 192.2 km from Dhaka. It can be accessed by both train and bus from the capital city Dhaka. Both mode of transport takes about 4 and half hours to reach there. 4.5 hours long bus journey. It can also be accessed from the Chittagong Divisional headquarters which is located about 56 km to the south of the Upazila and takes 1.5 hour travel by either bus or train. The Bangladesh Road Transport Corporation introduced a direct bus service from Dhaka to Mirsharai via Comilla (Source: Bangalapedia, 2012)

Mirsharai, the combination of lake and hilly area contains attractive scenic beauty on the southeastern part of Bangladesh. The most important attraction of the upazila is that one can travel Mohamaya Chara Lake by speed boat and explore hilly area and can enjoy Khoyachora, Baghbani, Napitachora, Sonaichora, Mithachora and Boyalia waterfalls.

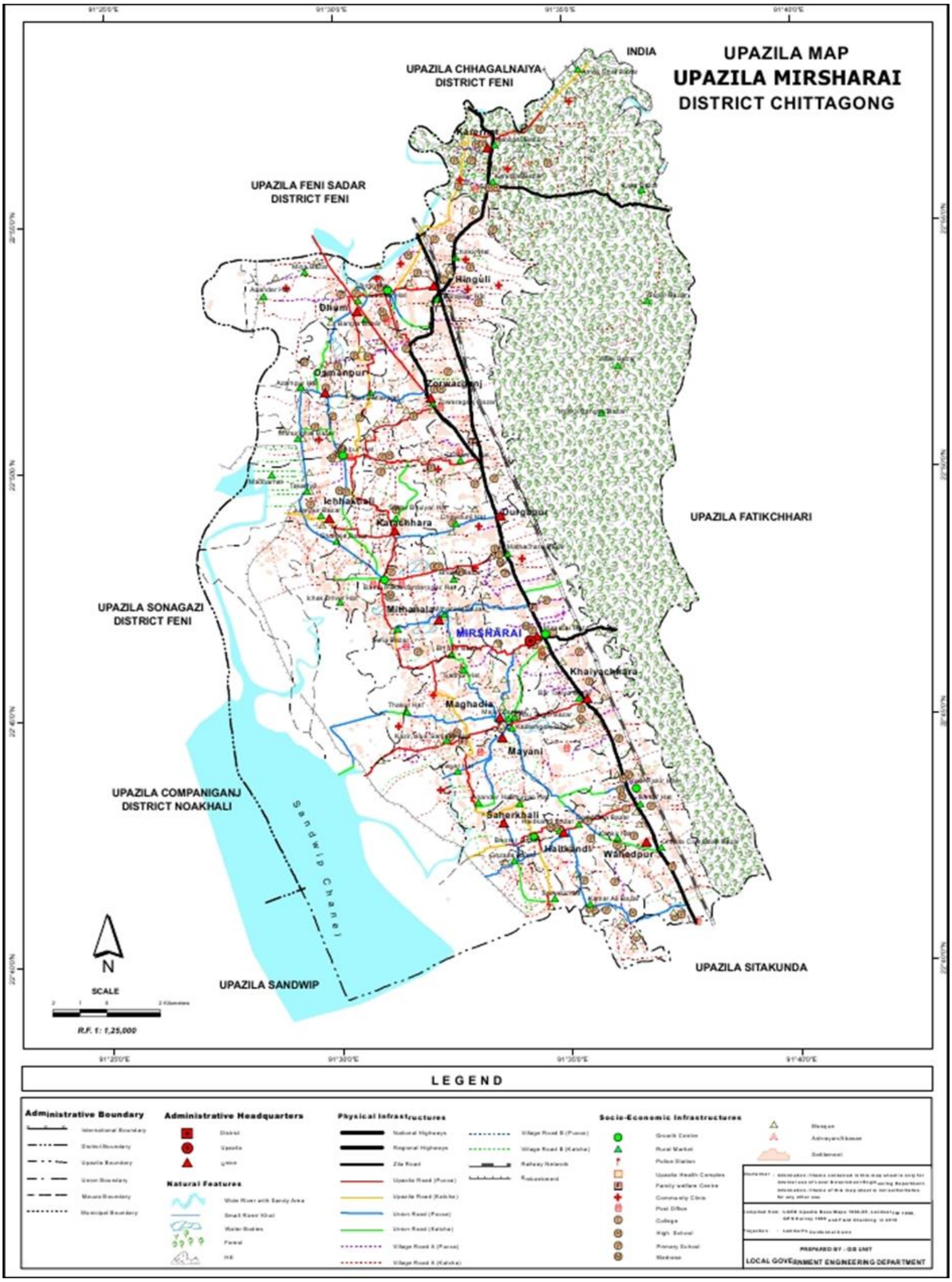

Figure 1: Map Showing Location and Accessibility (Source: LGED)

1.2. Topography and Relief

Topographically the Upazila contains both hilly areas and plain lands. Approximately, one half of the Upazila lies in the low lying hills of the Chittagong hill tracts in the east. The hilly region has high relief and is sparsely populated. The highest elevation in the hills is about a100 m and the lowest elevation in the hills is about 30 m. The western half of the area is plain lands with an average elevation of only about 5 m above mean sea level. This area is heavily populated. Numerous small streams crossed the hilly region and flows towards Sandwip Channel across the plain land (Figure 1).

2. Methodology

This study utilizes both field and laboratory procedures to assess the hydrological and hydrogeological conditions of the study area. Field study includes- a) drilling of boreholes at 5 locations for lithological sample collection for laboratory analysis as well as installation of monitoring wells, b) electrical resistivity survey, c) water quality survey including field measurement of important water quality parameters as well as sample collection for laboratory analysis, d) measurement of the depth to groundwater levels, and d) slug test to determine aquifer properties. Details of each of the above mentioned field activities are discussed in the subsequent sections.

2.1. Field Investigations

2.1.1. Drilling and Installation of Monitoring Wells

A total of 5 boreholes were drilled at different locations within the study area (Figure-2 and Table-1) for direct assessment of subsurface geological conditions with depth and space as well as to install wells to monitor groundwater level and water quality. Locations of the boreholes/monitoring wells were chosen carefully to ensure their distribution throughout the Upazila and to maximize the data coverage.

Table 1: Details of the boreholes and monitoring wells.

Borehole ID	Latitude	Longitude	Total Drilling Depth [m]	Screen Depth [m]
MW-01	22.88738	91.5546	219	165
MW-02	22.82665	91.48352	222	210
MW-03	22.78856	91.55094	204	195
MW-04	22.73395	91.50329	216	201
MW-05	22.70814	91.56847	159	156

Reverse circulation conventional drilling method was used in drilling the monitoring wells (Figure-3). Subsurface Geological variation with depth were recorded at each drilling locations during the time of the drilling by investigating the drilling cuttings at a regular interval of 3.0 m. The information was then recorded using a standard data recording format in Appendix-I. Additionally, the drilling cuttings were sampled at every 3.0 m and approximately 500 gm (Figure-3) of sample from each depth points were preserved in a polybag for transporting to a lab for grain size analysis.

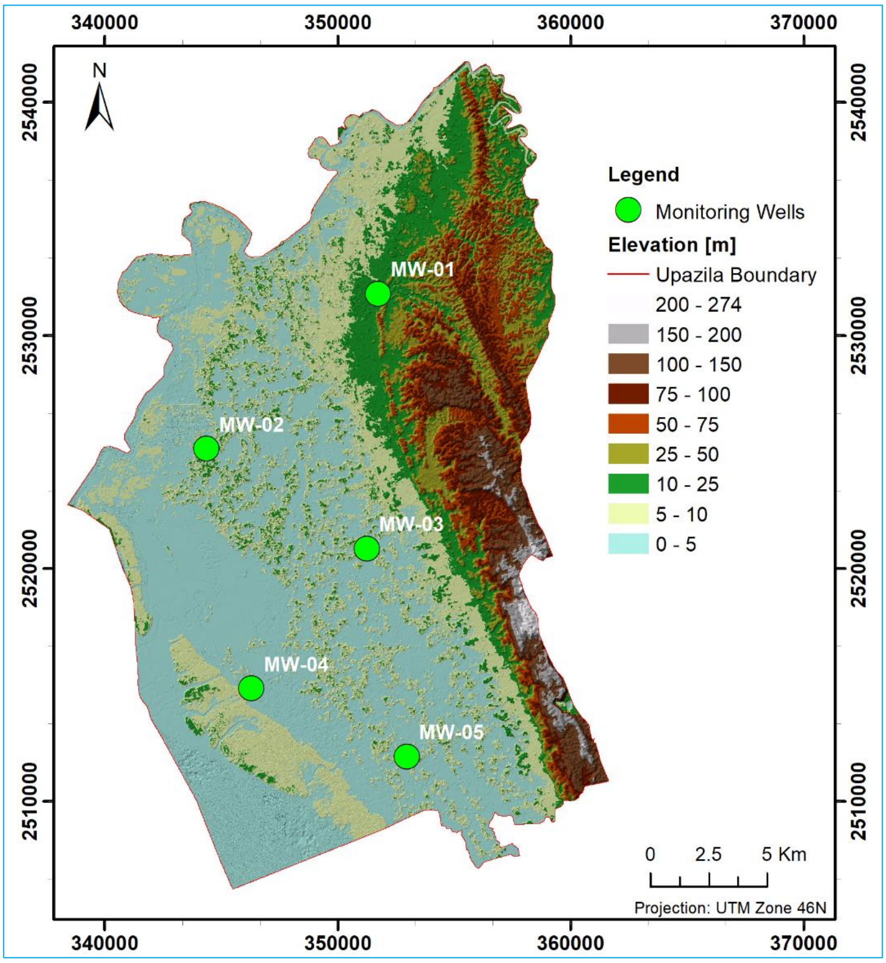

Figure 2: Digital Elevation Model of the study area (Source:UDD) along with the locations of the monitoring wells and drilling sites.

Monitoring well was installed at each borehole site. After careful investigation of the drillers log prepared during the drilling, a suitable aquifer zone was chosen at each site for well screen. At each location, 9.0 m long screen with 1.5 inches diameter were installed.

Figure 3: Monitoring well drilling and Wash samples.

The borehole depth interval between the top of the screen to the land surface was cased using 1.5 inches PVC pipe except in two locations. The exceptions were in areas where the water table was relatively deeper than other areas. In these locations 40.0 m long and 3 inches diameter housing were installed (Figure-4). After installation of a monitoring well it was washed properly following standard procedure. The standard lithological log is attached in Appendix-I.

Figure 4: Established Monitoring well with 3 Inches Housing Pipe.

2.1.2. Electrical Resistivity Survey

Vertical Electrical Sounding (VES) is by far the most used method for geo-electric surveying, because it is one of the cheapest geophysical method and it gives very good results in many area of interest.

The field measurements technique is adjustable for the different topographic conditions and the interpretation of the data can be done with specialized software, with a primary interpretation immediately after the measurements. The results of **VES** measurements can be interpreted qualitatively as well as quantitatively.

The principle of this method is to insert a electric current, of known intensity, through the ground with the help of two electrodes (power electrodes – AB) and measuring the electric potential difference with another two electrodes (measuring electrodes – MN) (Figure-5). The investigation depth is proportional with the distance between the power electrodes.

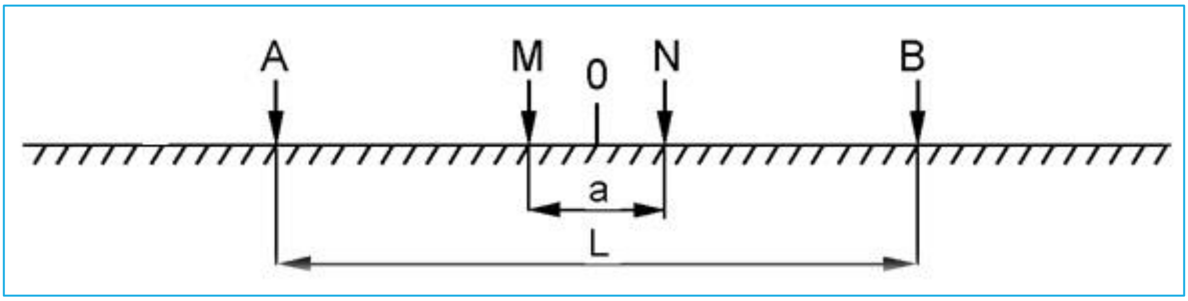

Figure 5: Schulumberger array of VES.

Since direct investigation of the surface geology by drilling boreholes is costly and usually done in widely distributed locations, the information gap in-between drill sites is usually fulfilled using various geophysical surveys. In this study vertical electrical sounding

(VES) method was used to deduce the subsurface lithological/hydrogeological variation with depth at a number of locations distributed all over the study area (Figure-6).

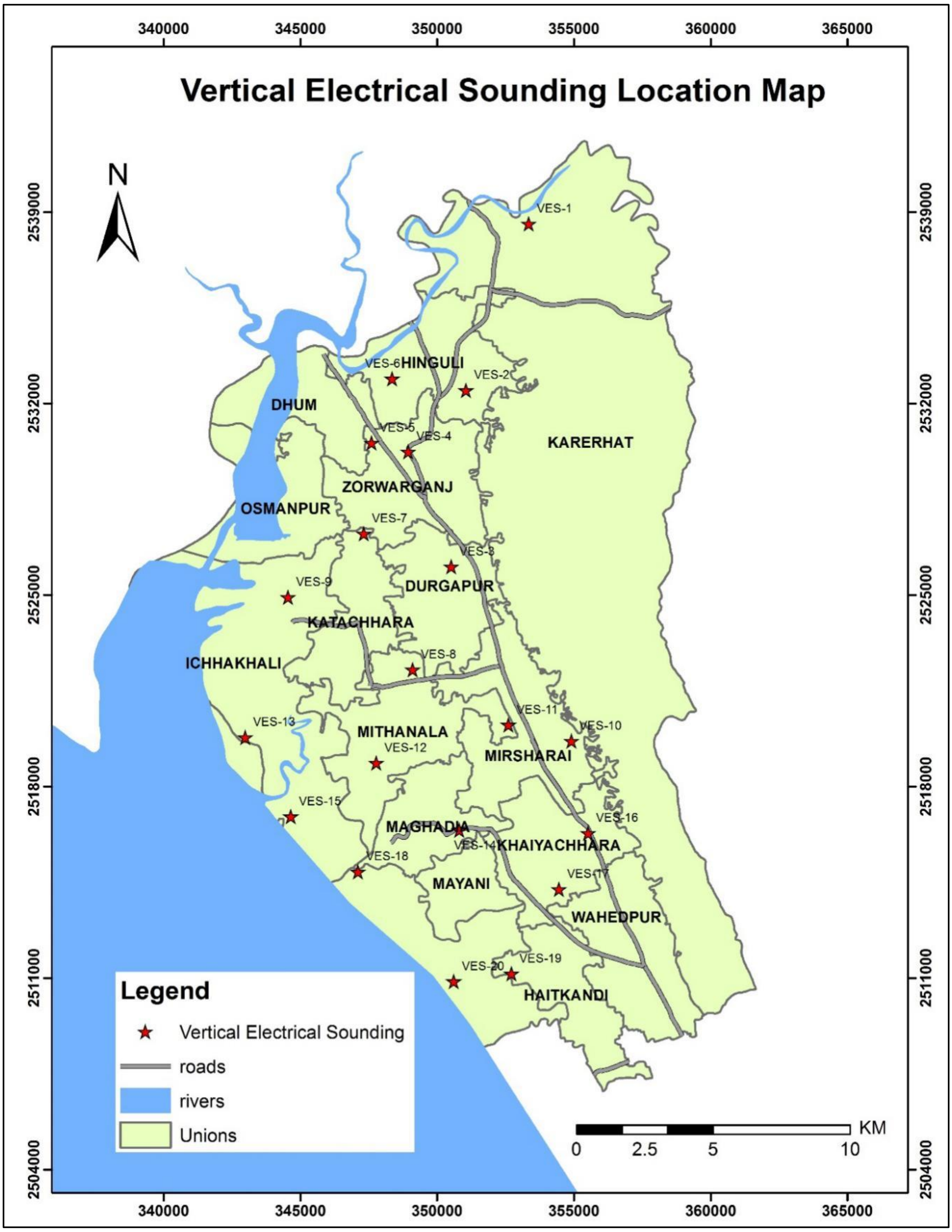

Figure 6: Vertical Electrical Sounding Locations in the project area.

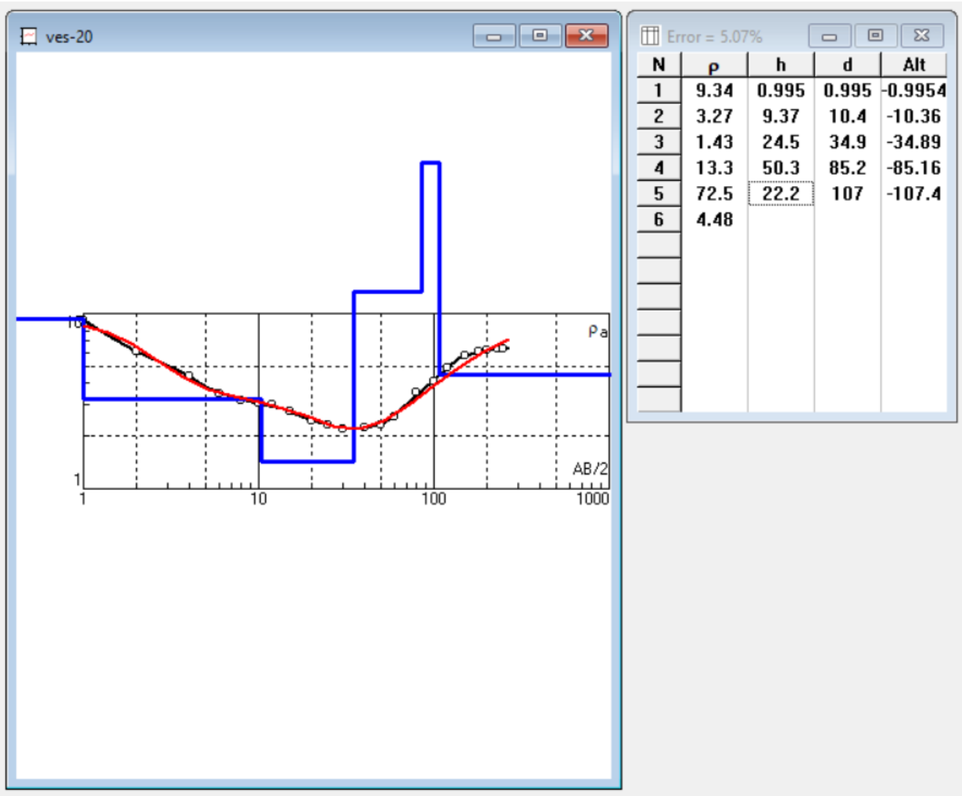

Figure 7: Sounding Curve VES 20 and the respective subsurface geo-electric model (Left), layer resistivity, thickness and depth to the right.

Rho [ohm-m]	Thickness [m]	Depth [m]	Lithology
9.34	1	1	Top soil
1.43-3.27	34	35	Brackish Sand
13.3	50	86	Clay
72.5	22	108	FW Sand

Table 2: Interpreted result for VES-20 obtained from geo-electric model

Raw data from field for VES, Sounding Curves and subsurface geo-electrical model as well as interpretation from geo-electrical model of rest of the VES are given in Appendix-II.

Figure 8: Resistivity Survey (VES) in Presence of UDD personnel and Local Pouroshova Commissioner.

2.1.3. Water Quality Survey and Sampling

A number of field parameters were measured in the field using field kits and handheld filed instrument at more than 76 locations including shallow and deep wells in the study area (Figure-9). At every location, at least two wells, one at depth shallower than 100 m and the other at depth deeper than 100.0 m were surveyed.

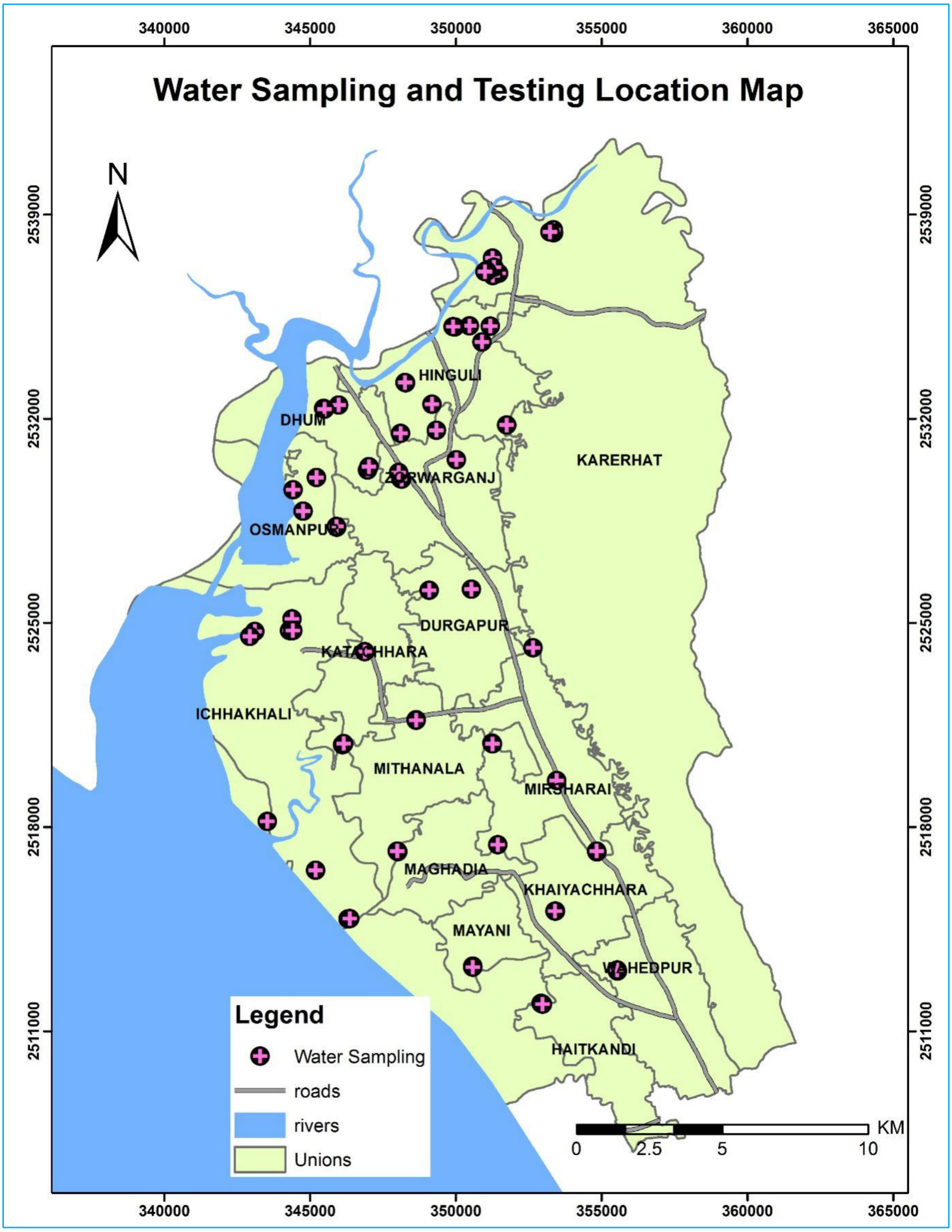

Figure 9: Water sampling and testing location map

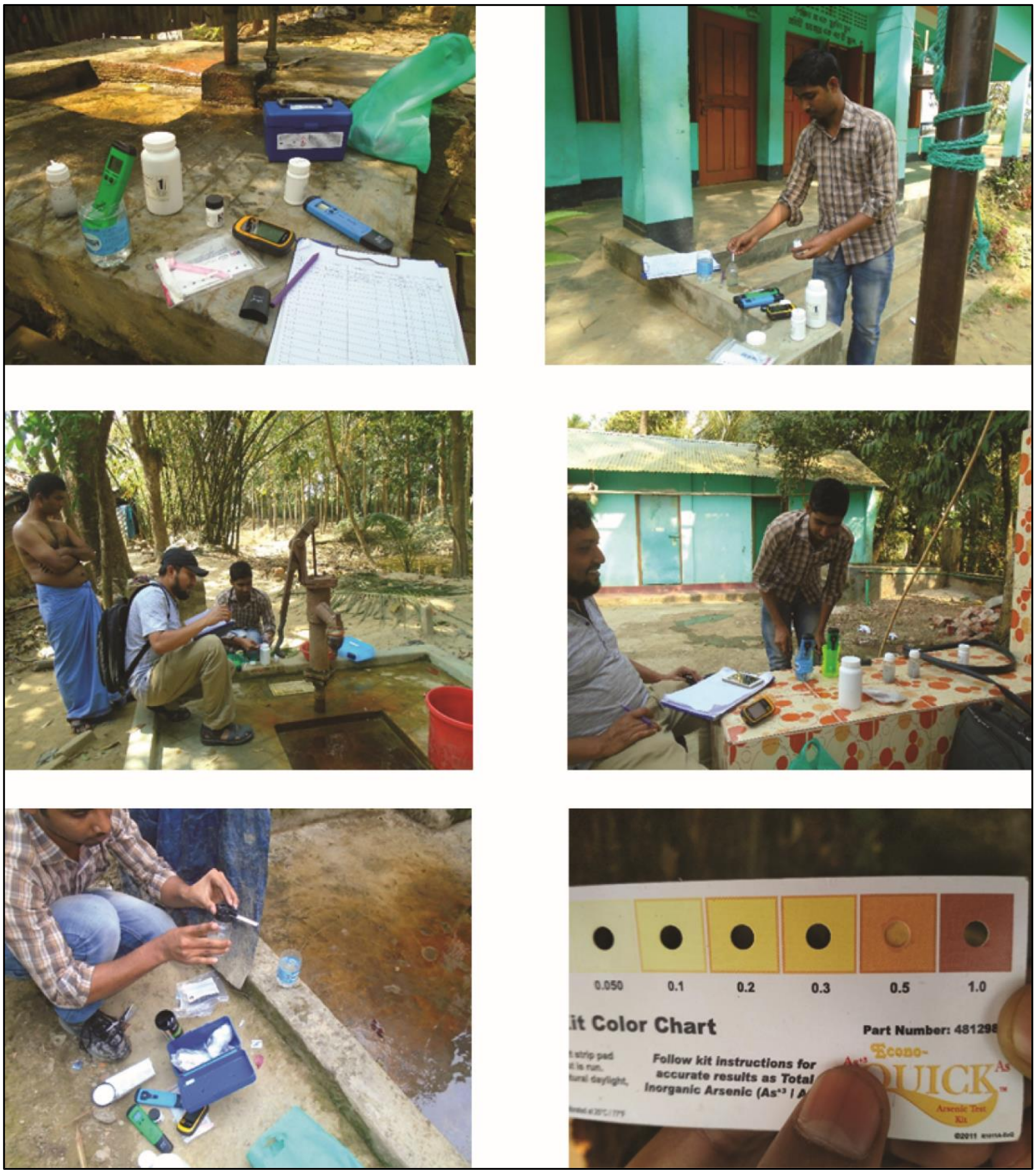

Figure 10: Water Sampling and Field Tests of Arsenic, EC, PH, EH, Temperature etc.

Water samples were also collected from these wells for detail chemical analysis in the laboratory. For each well, two samples each 125 ml and one acidified, was collected in plastic bottles. Each well was purged for at least 10 minutes before field measurements and sampling. The field parameters measured using handheld meters include- pH, Eh, EC, and Temperature. Arsenic was measured in the field using Econo-Quick™ Field kit. Details of the field data are given in Appendix-III.

2.1.4. Groundwater Level Survey

Depth to groundwater was measured in the filed using the Kaizen Imperial™ level meter at each of the water sampling locations (Figure-9). Like the water sampling, water level was measured in both a shallow and a deep well at every location except when the pair was not available. The depth to water data collected from the field was later converted to groundwater level with the help of the DEM supplied by UDD.

Figure 11: Water Level data collection in various location in Field.

2.1.5. Slug Test

Slug test was carried out in 22 locations almost uniformly distributed within the Upazila (Figure-10). During the test procedure a slug (2.0 m long iron rod of 0.75 inches diameter) was rapidly lowered in the well (after removing well head) (Figure-11). The slug displaces water in the well equal to its volume and caused the water level in the well to rise almost instantaneously and decays to its original position with time. Time required for the water level to reach its original position provides estimates of hydraulic conductivity of the aquifer zone surrounding the screen. An automatic water level logger was kept in the well before the slug was lowered. The logger recorded the changes of water level in the well with time. (Figure-12 & 13). The interpretation of slug test is given in Appendix-IV.

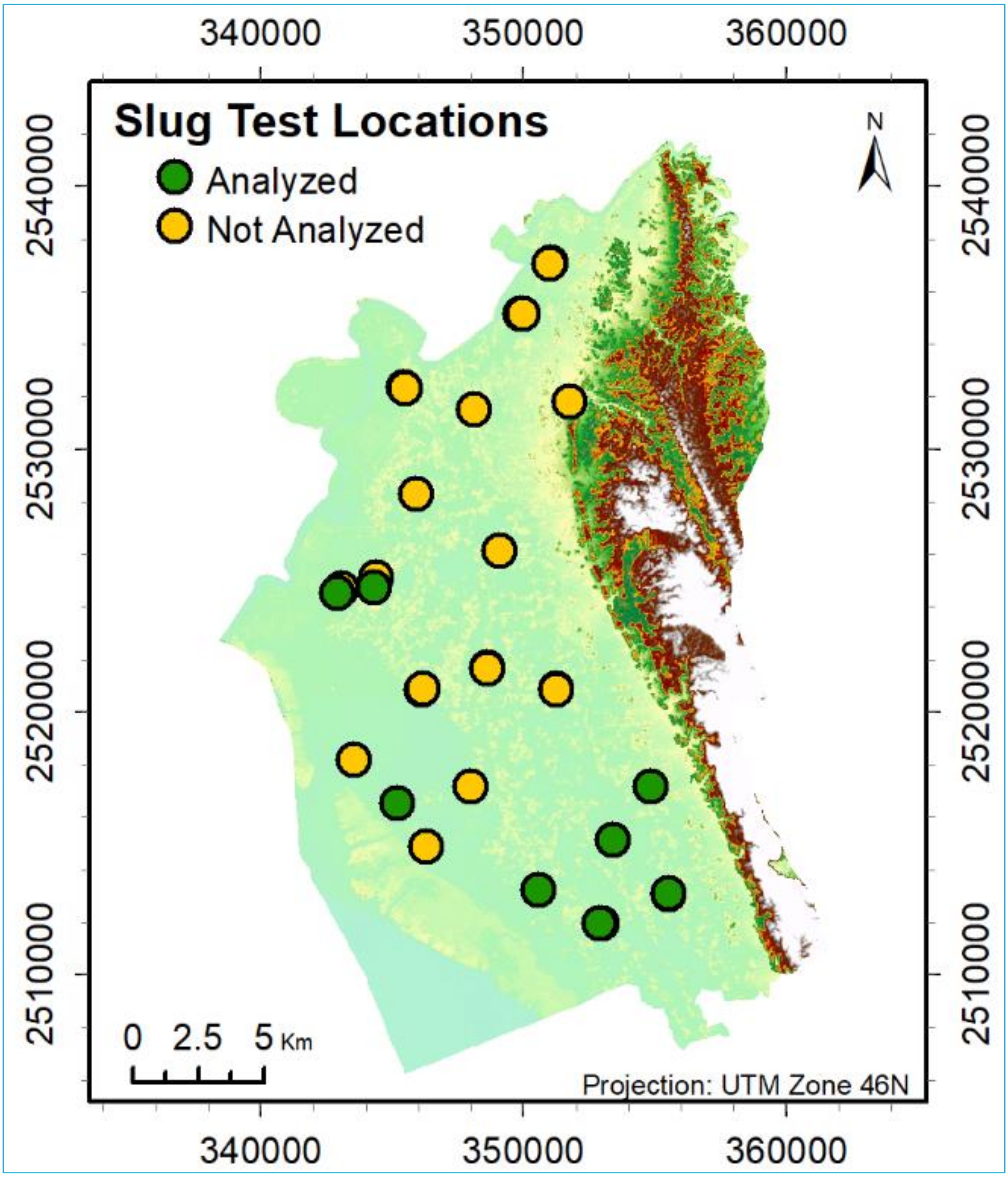

Figure 12: Map showing the locations where slug tests were carried out in the field. Most of the location has a pair of a deep and a shallow wells. Not all data have been analyzed yet, data points are highlighted for which hydraulic conductivity has been calculated from the field data.

Figure 13: Slug Test in field.

The Hvorslev equation (1) was used to analyze the slug test data for wells with overdamped response (Figure-14). A few wells showed underdamped response (Figure-15), slug test data for these wells were analyzed using Bouwer and Rice equation (2).

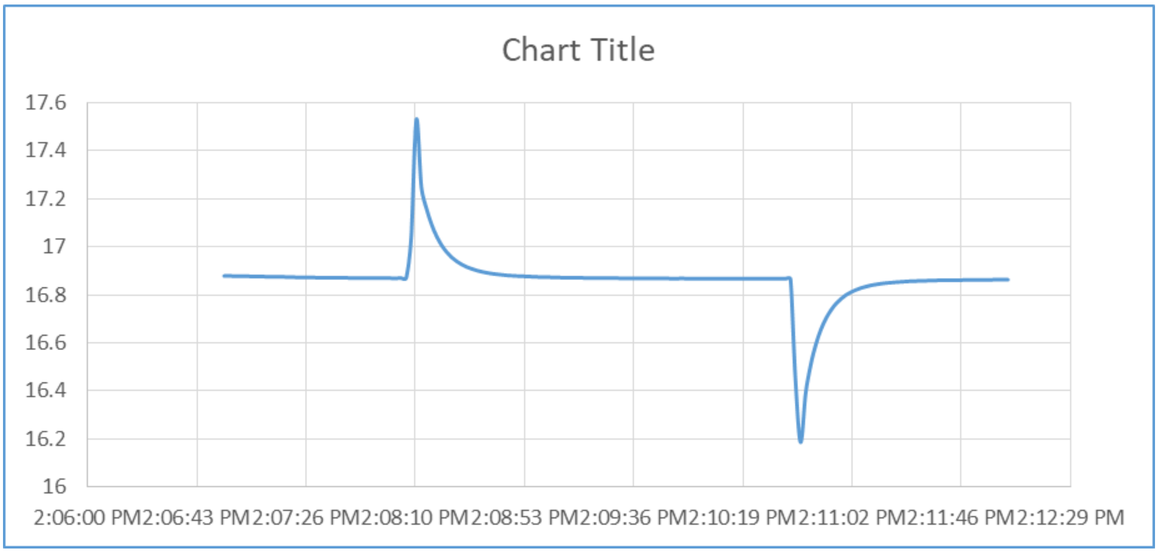

Figure 14: Overdamped Response.

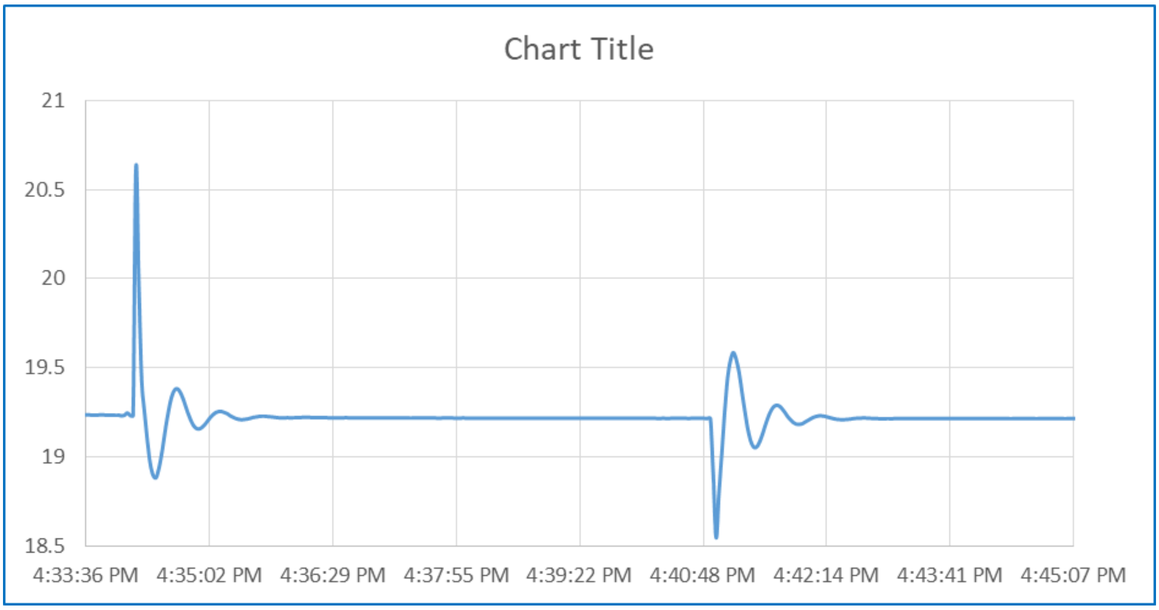

Figure 15: Underdamped Response.

Hvorslev Equation (1):

$$K = \frac{r_c^{\,2} \cdot \ln\left(\frac{L_e}{r_w}\right)}{2 \cdot L_e \cdot t_0}$$

where r_c is the radius of the well casing (m), L_e is the length of the well screen (m), r_w is the radius of the well screen (m), t_0 (s) is the basic time lag and the time value (t) is derived from a plot of field data. Generally, t_{37} (s) is used, which is the time when the water level rises or falls to 37% of the initial hydraulic head H_0 (m), the maximum difference respect the static level

Bouwer and Rice (1976) Equation (2):

$$K = \frac{r_c^{\,2} \cdot \ln\left(\frac{R_e}{r_w}\right)}{2L_e} \cdot \frac{1}{t} \cdot \ln\left(\frac{H_0}{H}\right)$$

where R_e is the radius of influence (m), and t is the time since $H=H_0$.
Using the results from an electric analog model, Bouwer and Rice obtained two empirical formulas relating $ln(R_e/r_w)$ to the geometry of an aquifer system, the first for $L_w>B$ and the second for $L_w<B$, where B is the formation thickness (m) and L_w is the static water column height (m).

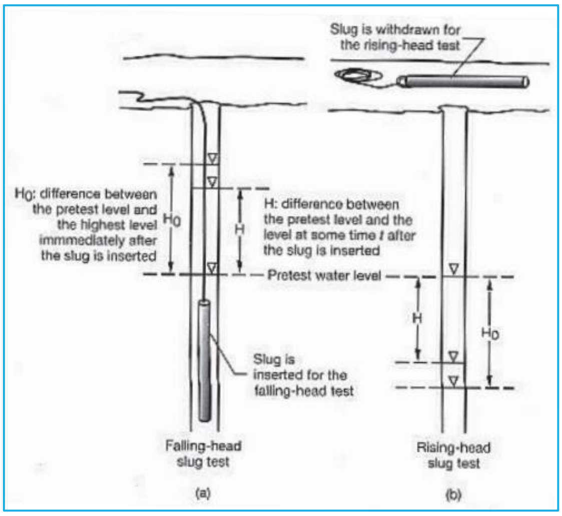

Figure 16: Slug Test Operative Method.

2.1.6. Identification of Surface Waterbody, Flash Flood zoning and mitigation approach

In Mirsharai Upazila Main River is Feni; Sandwip Channel is notable; Canal is about 30 nos, most noted of which are Feni Nadi, Isakhali, Mahamaya, Domkhali, Hinguli, Molisaish, Koila Govania and Mayani Khal. All the rivers and khals and canals are coming from eastern hilly region and falling in Bay of Bengal. In the high tide, sea water enter into the canal and go back into sea in low tide time.

At the monsoon season heavy rainfall occur. As the project area is bounded by hills at eastern side and west by sea, the rainwater influx affects the project area by flash flood. By discussing with local people it is very clear that flash flood effect is prominent in monsoon season. In this phase five (5) major basin/watershed were delineated which is shown in figure-17.

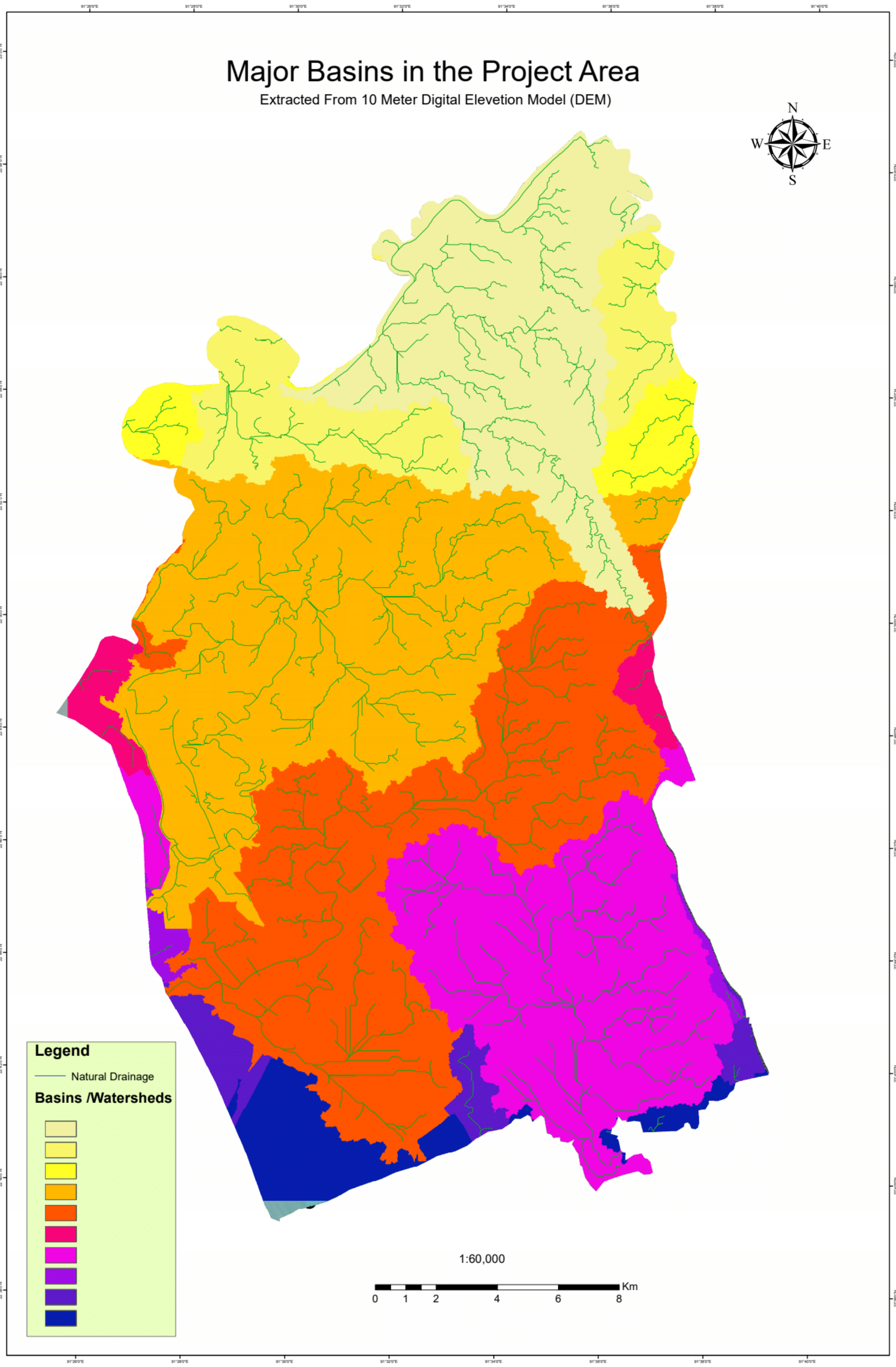

Figure 17: Major basin/watershed identified in the project area.

As the part of the study there was a scope beyond the ToR, to identify prospective artificial reservoirs for fresh water which can be the alternative source of water for irrigation as well as drinking and other uses. The prospective zones were identified (Figure-18) and labeled as prospect-1 to prospect-4. The existing Mohamaya Lake was also demarked to validate the prospect identified with the help of 10 m DEM supplied by the client.

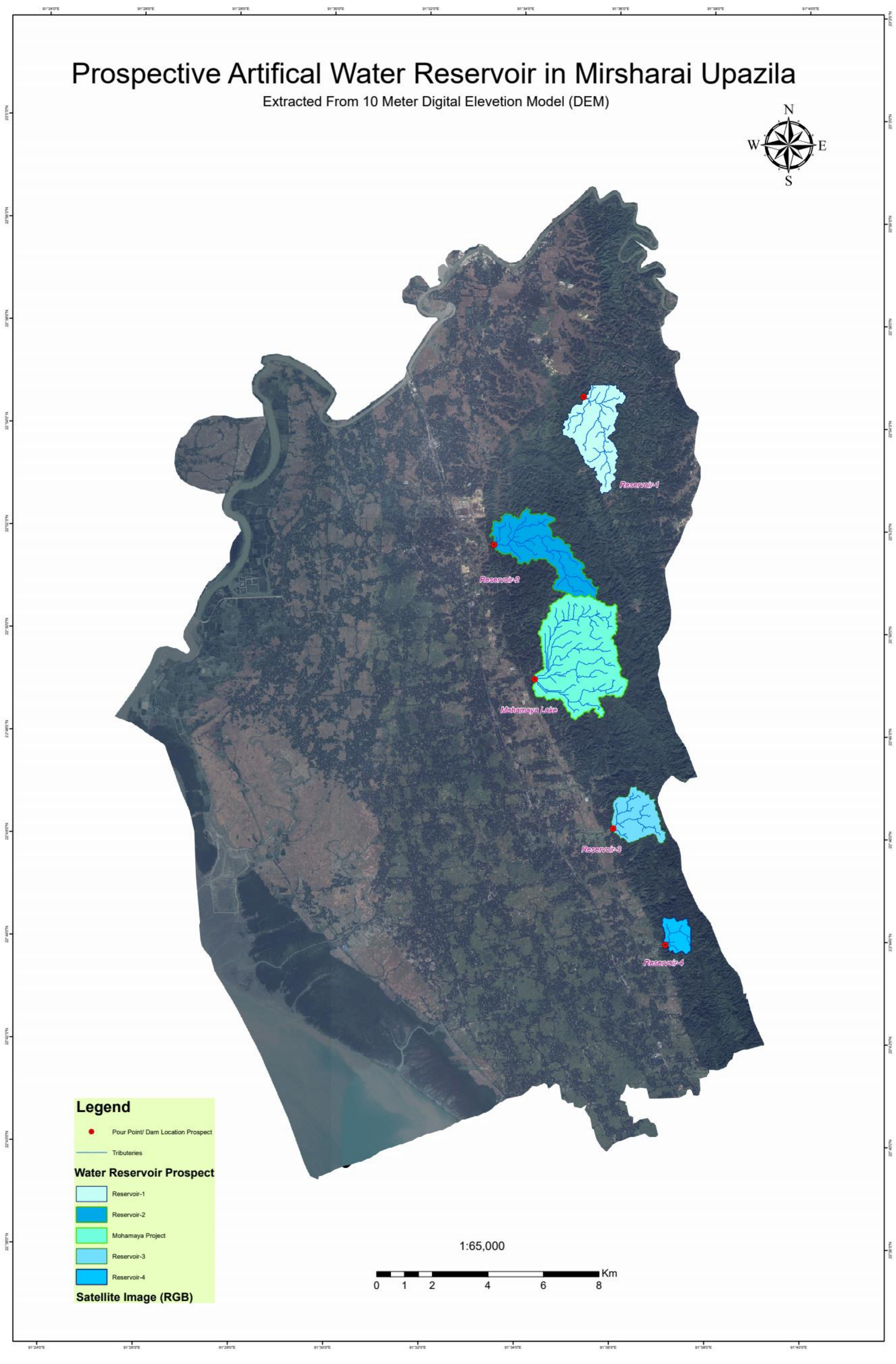

Figure 18: Prospective artificial reservoir locations

Surface waterbody maps, flash flood zoning and corresponding result of the project area will be provided after getting the Physical features survey data and verified DEM from UDD in the next phase of reporting.

2.2. Laboratory Analysis

2.2.1. Grain Size Analysis

Lithologic samples collected from the monitoring wells were sorted and depending on the lithological variability samples from each aquifer unit was selected for grain size analysis. Grain size analysis includes oven drying the samples and then sieving through various mesh sizes and calculation of weight percentage for different size fraction (Figure-19). Grain size data was later used in calculation of hydraulic conductivity of the aquifer unit using empirical formula.

In 1893, Hazen published his formula for estimating hydraulic conductivity:

$K = C_H \times D_{10}^2$

K = Hydraulic conductivity [m/s]

C_H = Empirical constant, in this study set to 0.01157 [-]

d_{10} = The particle size for which 10% of the material is finer [mm]

The Hydraulic Conductivity obtained from the grain size analysis of the samples from monitoring wells are attached in Appendix-V.

Figure 19: Grain size Analysis in Laboratory

2.2.2. Water Quality Analysis

Water samples collected from the field were brought to the laboratory for detail chemical analysis. Chemical analysis includes determination of the concentration of major ions and trace elements. All the samples were tested in the laboratory. The water quality data are given in Appendix-VI. List of chemical species and analytical methods are given in Table -3.

Serial no.	Chemical constituents	Methods and Instruments
1	Sodium (Na+)	Atomic absorption spectrometer(GBC sens AAS)
2	Potassium (K+)	Atomic absorption spectrometer(GBC sens AAS)
3	Calcium(Ca2+)	Atomic absorption spectrometer(GBC sens AAS)
4	Magnesium(Mg2+)	Atomic absorption spectrometer(GBC sens AAS)
5	Bicarbonate(HCO3-)	Titration method (standard H2SO4 for HCO3-)
6	Chloride(Cl-)	Titration method (standard AgNO3 for Cl-)
7	Nitrate(NO3-)	UV visible spectro-photometer(wave length 410nm)
8	Iron (Fe)	Atomic absorption spectrometer(GBC sens AAS)
9	Manganese (Mn)	Atomic absorption spectrometer(GBC sens AAS)
10	Arsenic (As)	Atomic absorption spectrometer(GBC sens AAS)
11	Sulphate(SO42-)	UV visible spectro-photometer(wave length 410nm)

Table 3: List of chemical species and analytical methods

2.3. Groundwater Modeling

A three dimensional groundwater flow model has been developed using the USGS finite difference flow code MODFLOW. The model consists of 345 rows and 210 columns, each 100 m in length and width, respectively, resulting in a total number of 72450 cells per layer (Figure 20). There are a total of 6 layers in the model representing three aquifers, two aquitards, and a thin low permeability layers at the top. Thickness and depth of each layer varies from place to place as depicted from the 3D lithological modelling.

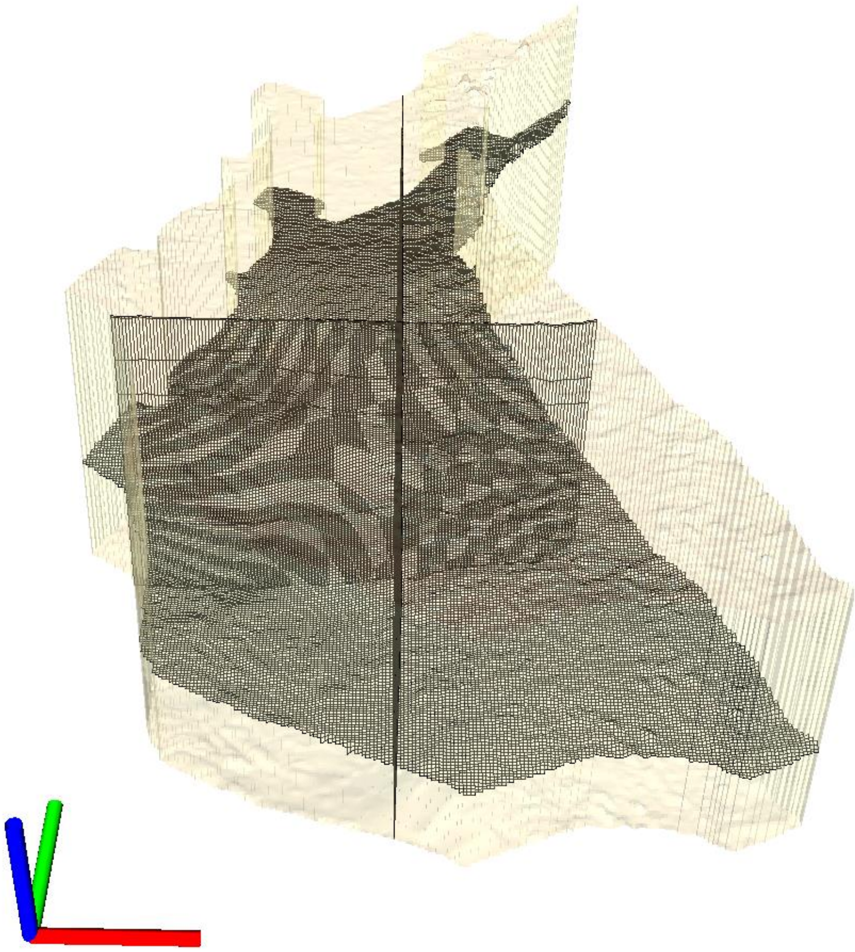

Figure 20 Groundwater Model Setup and discritization

The left boundary of the model is represented by constant head in response to the presence of the Feni River in the north west, and the Sandwip Channel in the West, South West. Head along the Feni River is approximated to be decreasing from north to south following the same gradient as the land surface elevation along the river. Head for the Sandwip channel is considered to be zero since this is located very close to the sea. The southern boundary of the model is represented by another constant head boundary, the head value along this boundary is based on the head measurement from the field. The eastern part of the study area is bounded by hills, therefore, it was represented by a no-flow boundary condition in the model. At the bottom of aquifer three there is a clay layer ubiquitously present in the study area, therefore, the bottom boundary of the model also represented by a no-flow boundary. The top boundary was approximated using a constant value of recharge along with a drain allowing the model to accept as much recharge as required and reject the access recharge water through the drains. This trick was applied in the modeling because field estimation of groundwater recharge is difficult and never gives a reliable estimate. The model was run in steady state condition.

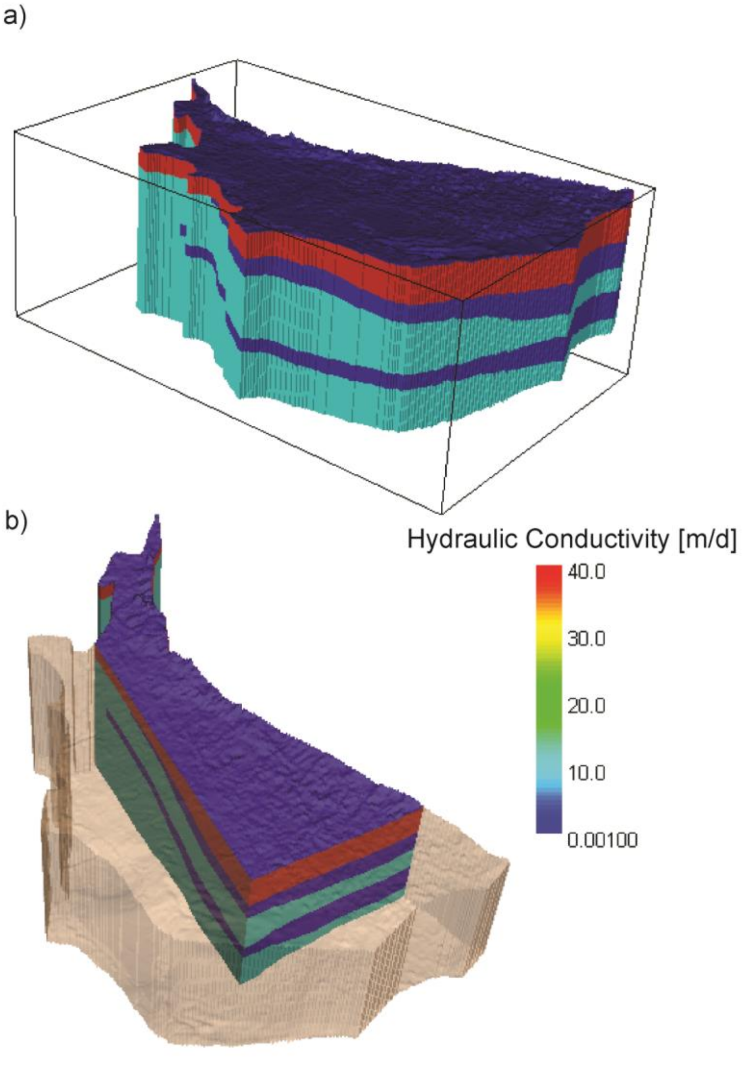

Figure 21: Model layers and their hydraulic conductivities

Hydraulic conductivity values that were estimated from slug test and grain size analysis for different aquifer layers were assigned in the model. It should be noted that the hydraulic conductivity is scale dependant, meaning its value depends on the scale of measurement. Usually, small scale measurement tend to underestimate it. Both slug test and grain size analysis provides estimate on a scale of cm to m, therefore, the estimated values are the lower estimate (Table:4). The modeling began with the exact value of the field estimated average value of hydraulic conductivity for each layer and later these parameters were to obtain a match of the simulated head data to the observed head data. It should be noted that the observed head data is highly affected by the topography and elevation of the well head, due to poor data on topography the exact match between the simulated head and the observed head is not possible. Therefore, emphasis was given to match the overall trend in flow direction and the ranges of head values between the observation and model simulation.

3. Result

3.1. Groundwater Resources

3.1.1. Aquifer Framework

Aquifer framework in the study are has been delineated based on the interpreted VES data, borehole logs from the five monitoring wells, and additional 4 borehole logs from the Department of Public Health Engineering (DPHE) located in the study area. At ecah location of borehole and VES, lithological data has been grouped into layers of aquifers and aquitards based on lithological characteristics and similarities. Available data indicate that there are three aquifers present in the study area separated by two aquitards. The depth and thickness of each aquifer varies considerably from place to place.

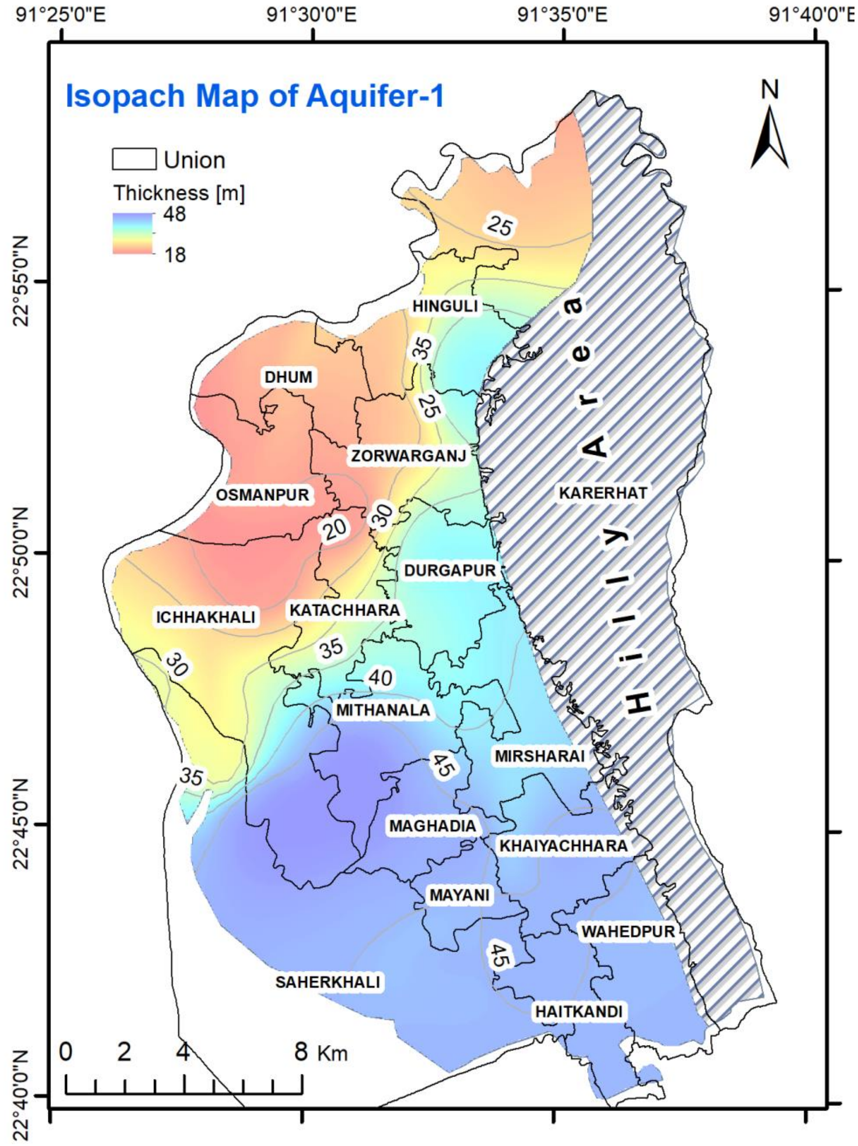

Figure 22: Isopach map of the shallow (1st) aquifer

The shallowest aquifer occurs at the surface and extend down to a depth of 20 to 45 m. The thickness of this aquifer is greatest towards the south and least towards the north and north west (Figure 22). Except the central part of the study area, the aquifer is exposed all over the study area below a very thin soil layer. In the central part of the study area the aquifer lies beneath a 5-7 m thick clay layer.

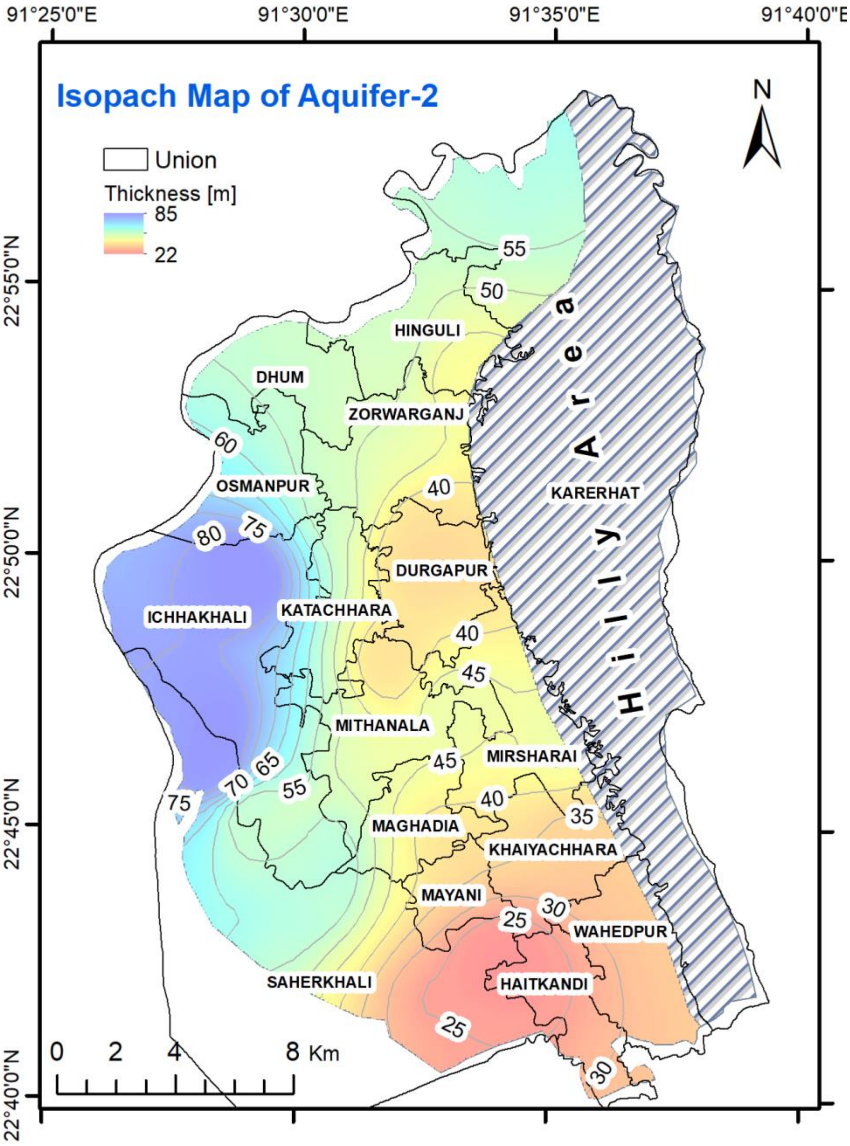

Figure 23: Isopach map of the second (intermediate) aquifer.

The second aquifer is 25 to 85 m thick and is separated from the first aquifer by an aquitard of variable thickness. The second aquifer is thickest in the west and thinnest in the south. In the north the aquitard is absent and both the first and second aquifers are connected. The aquitard separating the first and shallow aquifers are thickest in the south, about 50 m and absent in the north (Figure 24).

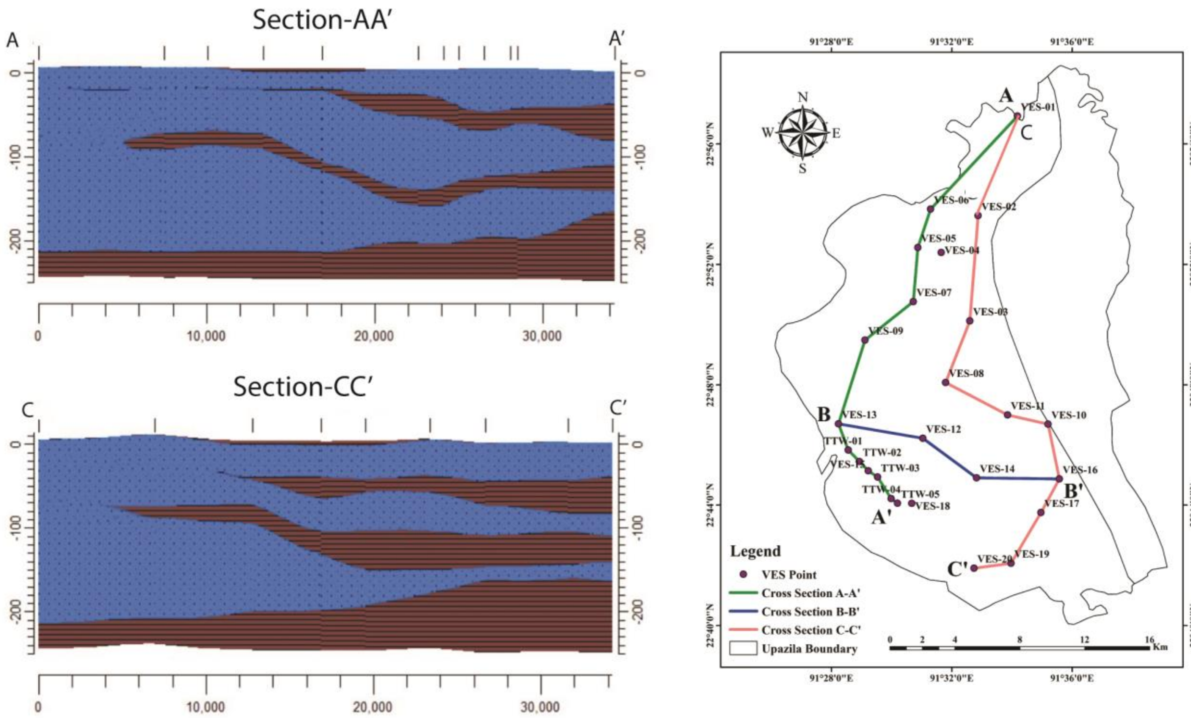

Figure 24: Cross section showing the vertical distribution of aquifer and aquitards in the study area

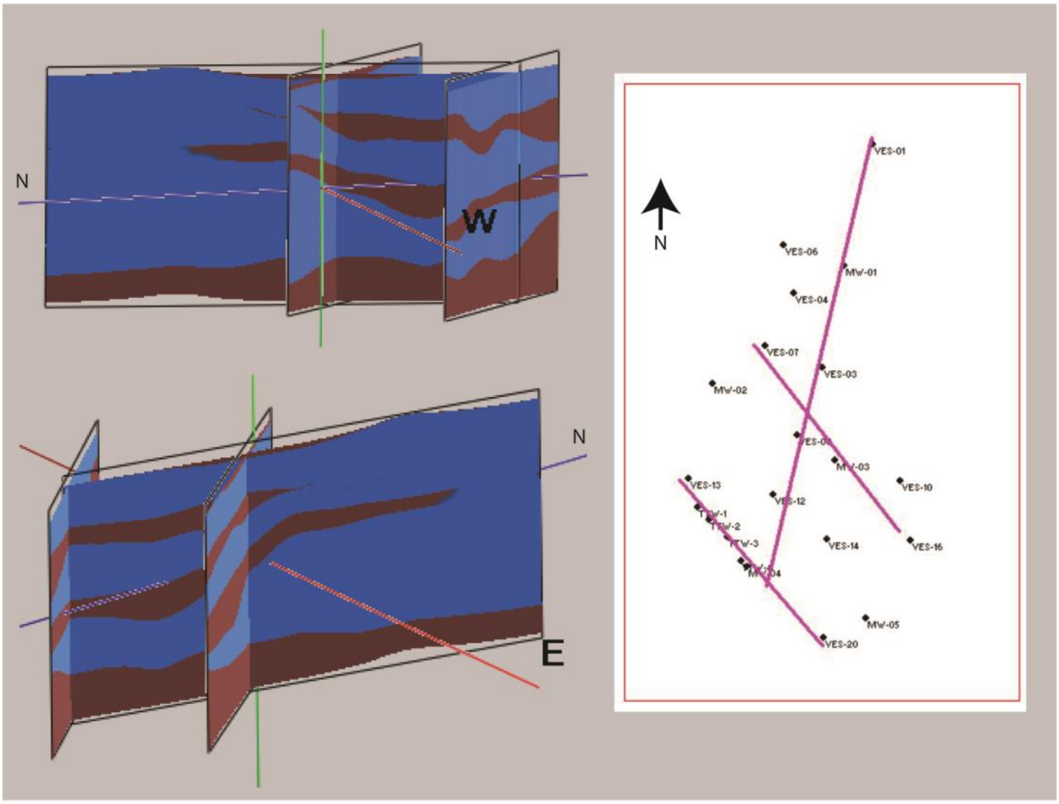

Figure 25: Fence diagram showing aquifer framework in the study area

The third or deep aquifer occurs around 100 m depth in the north and below 150m depth in the south. The aquifer is thinnest in the south and south east (20 m) and thickest in the north and north west (80 to 120m) (Figure 26). It is separated from the second aquifer by a 30-50 m thick aquitard in the south but connected with the second aquifer in the north (Figure 24 and 25). The thickness of the In fact, in the north the distinction between first, second, and third, aquifer is somewhat arbitrary as all these aquifers are connected to make only a single and very thick aquifer.

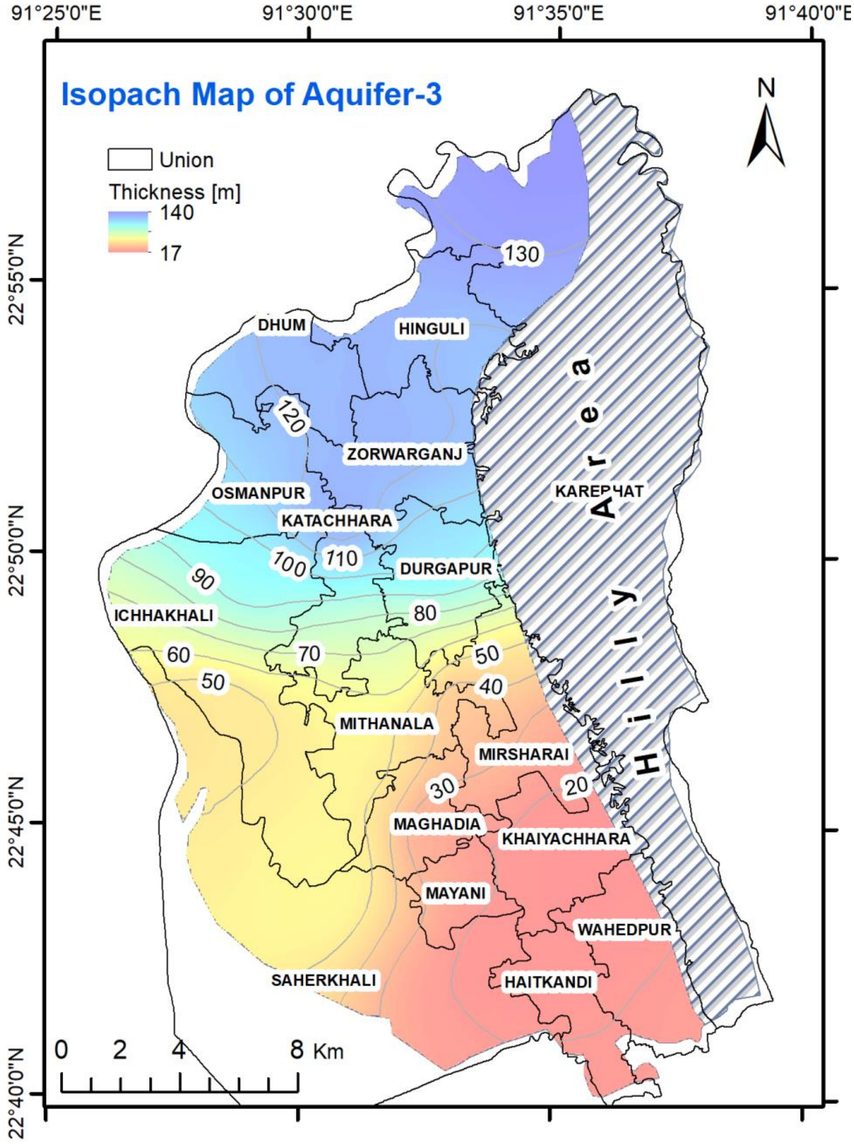

Figure 26: Isopach map of the deep aquifer

A three dimensional model of the aquifer architecture is produced using Rockworks software (Figure 27). This aquifer architecture provide the basic framework for the groundwater model. Layers shown in this model are included in the groundwater flow model. Hydraulic conductivity of each layer is estimated based on the interpretation of the slug test data and empirical equation derived estimate based on the grain size data. Hydraulic conductivity values for each layer are summarized in Table-4.

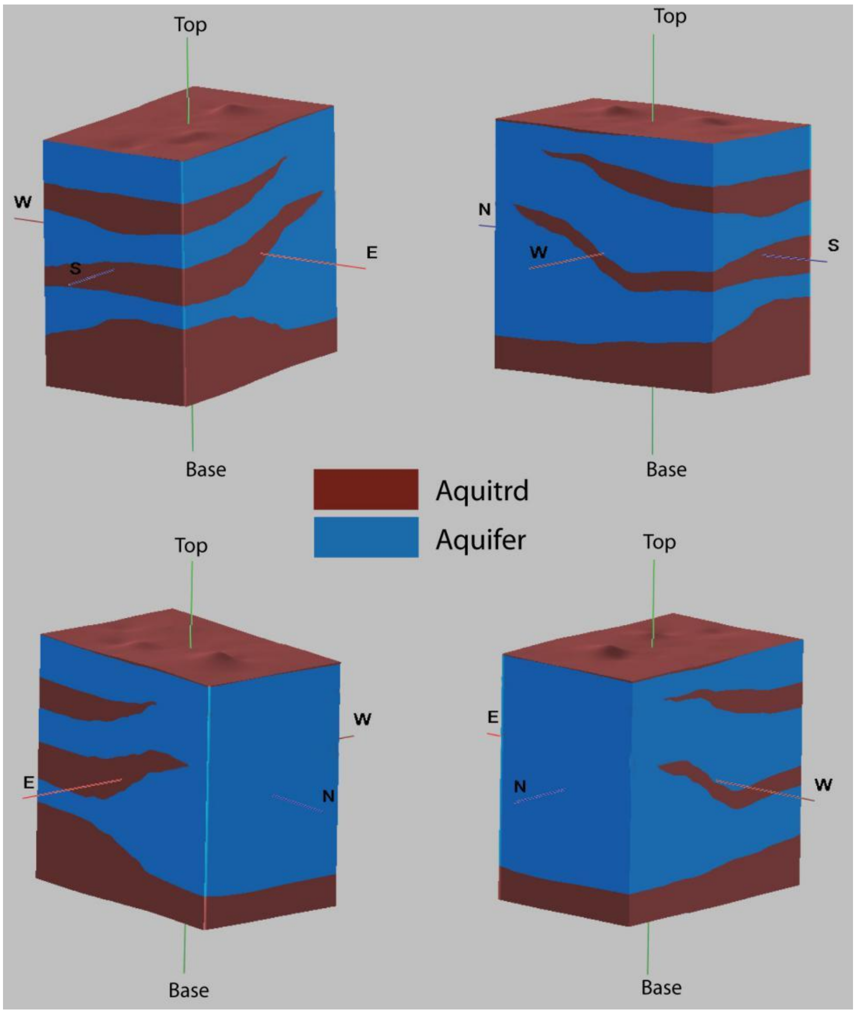

Figure 27: 3D model of aquifer architecture

Aquifer No.	Method							
	Slug Test				Grain Size Analysis			
	No. of Data	K [m/d]			No. of Data	K [m/d]		
		Average	Min.	Max.		Average	Min.	Max.
Aquifer-1	5	6.61	0.87	9.3	33	5.82	1.6	19
Aquifer-2	Nill	-	-	-	34	4.6	0.5	22
Aquifer-3	6	4.75	1	8.45	32	1.15	0.5	4.2

Table 4: Hydraulic properties derived from Grain Size analysis.

3.1.2. Groundwater Flow Direction

Groundwater flow direction was determined based on the field measurement of depth to groundwater level. The depth data was later converted to groundwater elevation based on the DSM supplied by UDD.

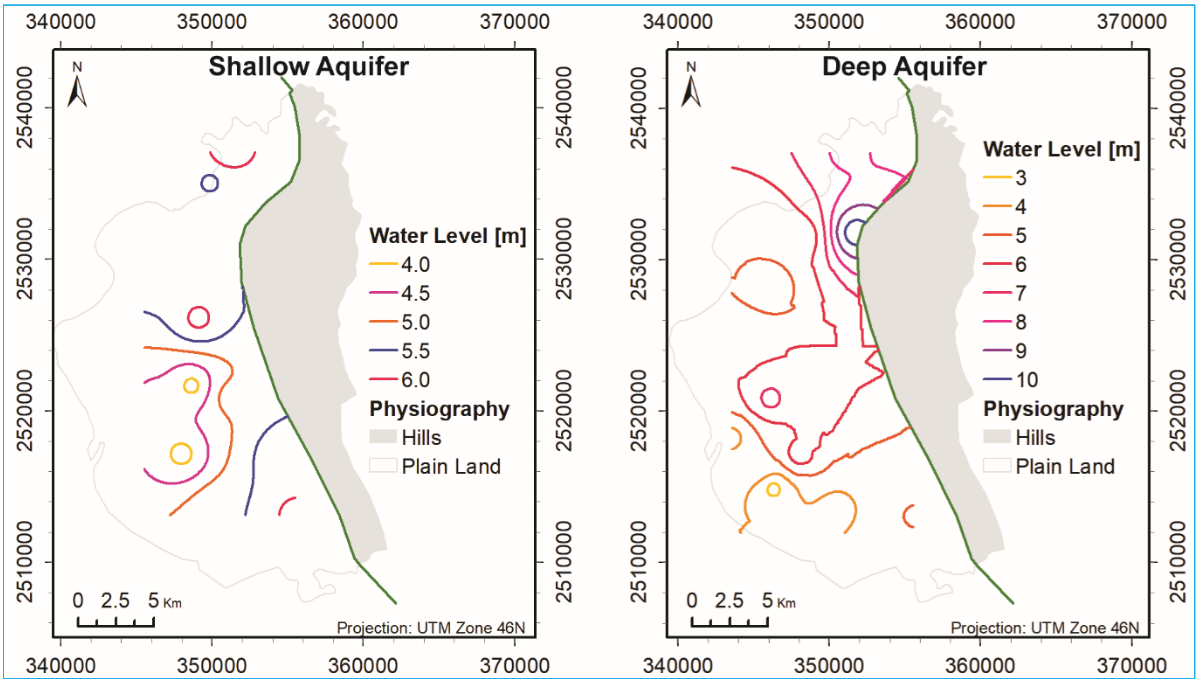

Figure 28: Groundwater level contour in the study area of the shallow aquifer and deep aquifer.

Figure-28 shows the groundwater level for both the shallow and deep aquifer. Groundwater level in the shallow aquifer varies between 4 m and 6 m. Though the data are very patchy, some regional trend in flow direction can be deduced from the figure. Generally, head is higher in the north and northeast and then that in the south and southwest. Groundwater flows from the north-northeast to south-southwest direction. The patchiness in the data is most likely due to inaccurate topography data together with uncertainties in the platform height of the wells. Groundwater level data for the deep aquifer is comparatively more coherent than the shallow data. There is a strong trend in groundwater level, groundwater flows from NNE to SSW direction.

It is worth noting that artesian flow has been observed in the field in the extreme north corner of the study area (Figure-24). Only the deep (>250 m deep) aquifer in that location flows automatically with an approximate head of 5 m above the land surface.

Figure 29: Artesian well the north-eastern part of the Project area.

3.1.3. Groundwater Quality

3.1.3.1. Major ions

Water chemistry data was analyzed in the lab in the department of geology university of Dhaka using spectrophotometry. All the water samples were grouped in to shallow and deep aquifer samples and the analyzed samples were plotted in piper diagram for both groups (Figure-30). Figure 30 shows that the water of the shallow aquifer ranges from $MgCO_3$-HCO_3 type to NaCl type. The $MgCO_3$-HCO_3 water type is found in the north and usually indicates recently recharges water, while the NaCl type water is found in the south indicating seawater intrusion. In the central part of the study area water samples indicate mixing between these two end members.

In contrast to the shallow aquifer, water of the deep aquifer are mostly Ca-K-Mg-CO_3-HCO_3 indicating unaffected by seawater intrusion. However, the line extending from Na/K towards Mg indicates ion exchange within the aquifer, which is a common natural phenomena and indicating longer residence time of water.

a) Shallow/First aquifer

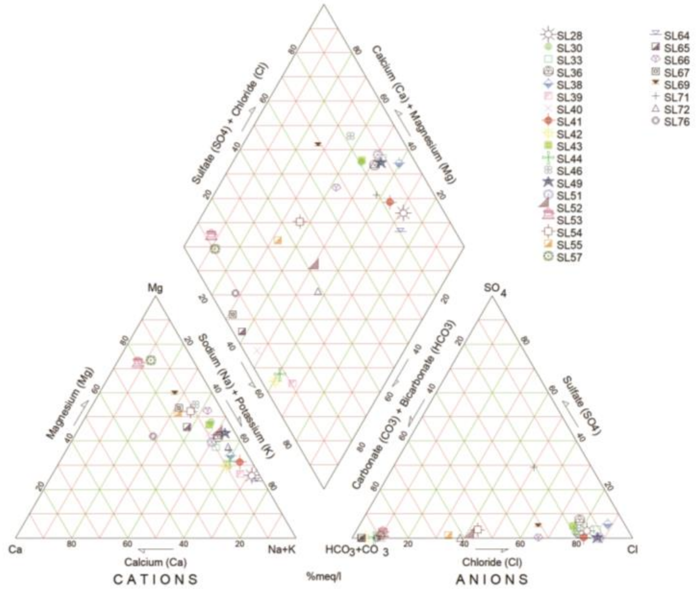

a) Deep/Third aquifer

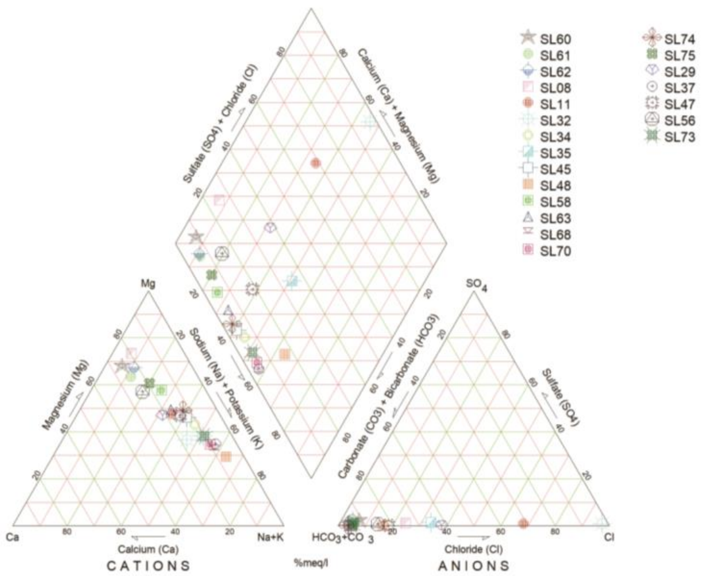

Figure 30. Piper diagram showing the major ion chemistry of a) shallow aquifer sample, and b) deep aquifer water samples.

3.1.3.2. Salinity/Electrical Conductivity

Electrical conductivity (EC) in groundwater is a measure of salinity and can indicate seawater intrusion or similar phenomenon. The EC in the shallow aquifer varies between 500 µS in the north to more than 8000 µS in the south and south west near the Sandwip Chanel. While, the groundwater in the deep aquifer is very fresh throughout the region with maximum EC value of 900 µS encountered in the extreme south. The EC value is exceptionally low (<200 µS) for both the shallow and deep aquifers in the northern tip of the study area.

The brackish water zone in the shallow aquifer is also picked clearly by the VES data (Figure 31). The lowest resistivity value is found between 20-50 m depth intervals in the resistivity pseudo profile, indicating the depth interval where the brackish water occurs. The low value below this depth is due to the influence of low resistivity at this depth and is not due to the presence of brackish water. Both the resistivity profile and EC contour indicate that only the shallow aquifer contains brackish water in the south, the second and third (deep) aquifer contain fresh water and can be used for drinking purpose.

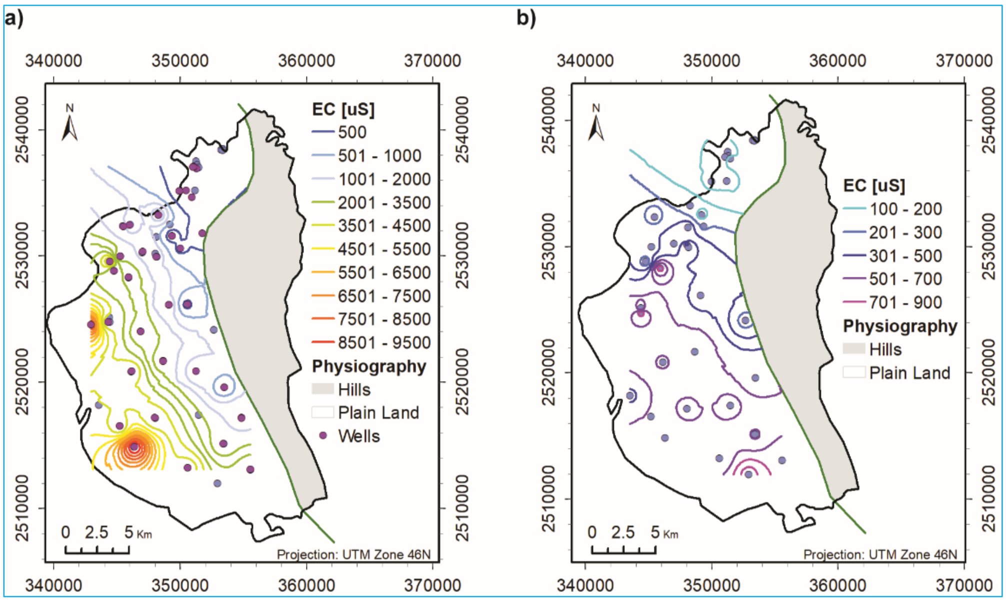

Figure 31: Map showing the spatial variability of electrical conductivity in the (a) shallow and (b) deep aquifer, respectively.

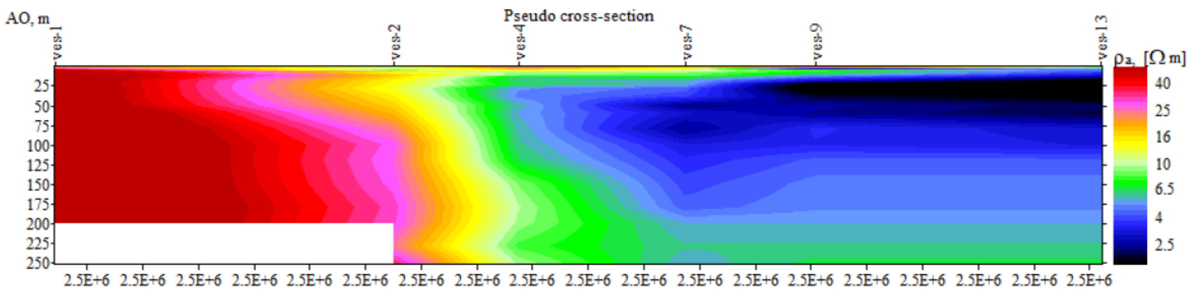

Figure 32. Resistivity pseudo section in north (VES-1) to south (VES-13) direction showing the extent of the brackish water in the shallow aquifer. For location of VES see Figure-6.

The EC contour at the shallow aquifer align perfectly with the orientation of the Sandwip channel, indicating that the channel is well connected with the shallow aquifer in this region resulting in the intrusion of saline water from the channel to the shallow aquifer.

3.1.3.3. Arsenic

Field kit measured arsenic concentration in a number of wells distributed within the study area are shown in Figure-26. Field kit data suggest that the shallow aquifer is heavily contaminated with elevated arsenic concentration throughout the Upazila except in the extreme northern corner. However, the deep aquifer is largely low in arsenic concentration except one or two locations. In these locations it is highly likely that the sampled wells are actually shallower than reported, depth verification is required before making any conclusion on the arsenic contamination of the deep aquifer in the study area. Moreover, field kits only provides indication of the likelihood of contaminated wells. Without laboratory analysis confirmation about the arsenic status for the deep aquifer where only a few samples show marginally high concentration would not be accurate.

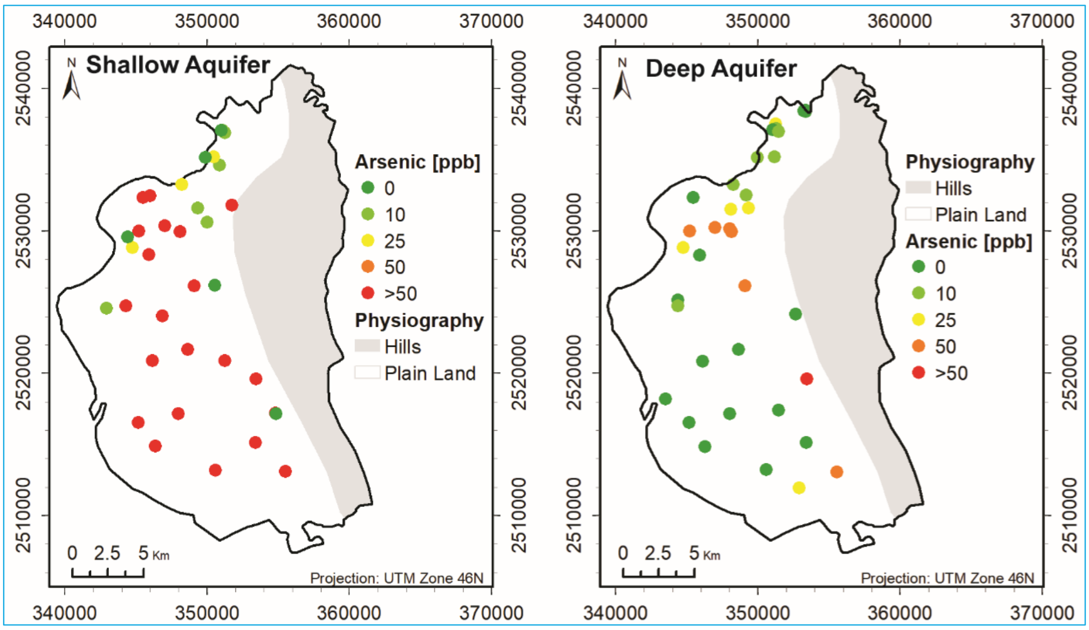

Figure 33: Arsenic distribution of Shallow and Deep Aquifer of the project area.

3.1.1. Groundwater Recharge Areas

Some preliminary assumptions about the groundwater recharge locations in the study area can be made based on the field observations. Groundwater level is the most important dataset delineating recharge zone, however, because of the erratic nature of the groundwater level data of the shallow aquifer it is really difficult to conclude anything based on groundwater level data for the shallow aquifer. However, the EC map provides a nice indication of the groundwater recharge areas as well as groundwater flow direction for the shallow aquifer. In recharge areas, the EC values are expected to be exceptionally low, and an increasing trend in EC from recharge areas towards discharge area is expected. Figure-23 (EC map) clearly suggest that the shallow aquifer receives most of its recharge in the northern part of the study area. This assumption is also supported by the arsenic concentration data. High arsenic is expected in old reduced water while there should be little or no arsenic in newly recharged oxidized water. The arsenic map of the shallow aquifer suggest that the norther part of the study area have very low arsenic concentration.

The groundwater level map of the deep aquifer readily indicates the location of the recharge area. It is also located in the north. Presence of artesian flow in some areas also indicates that some part of the deep aquifer must be exposed in the hills in the north where they receives bulk of the recharge.

The above discussed assumption has been verified using the groundwater model and found to be largely supported by the model. Figure 34 shows the distribution of model simulated recharge rate in the study area. The high recharge rate in the north is readily evident. However, the figure also indicates high recharge rate along the western boundary near the rivers and along the elevated eastern boundary. The high recharge rates along the western boundary is due to its location near a river, water infiltrates in to the shallow subsurface and quickly discharges off in to the nearby river. This recharge do not penetrate deeper in to the aquifer. Similarly, due to the presence of thick aquitard below the shallow aquifer along the eastern boundary, recharge along this elevated areas only add water to the shallow aquifer. In contrast, since all three aquifers are connected in the north and there is now aquitard present in between them, recharge in this region add water to all three aquifers. The deep aquifer which provides suitable drinking water throughout the upazila is primarily recharged in the north. Additionally, the deep aquifer could also be recharged regionally in areas farther north. Flow in to the deep aquifer from the constant head boundary in the northwest would indicate this.

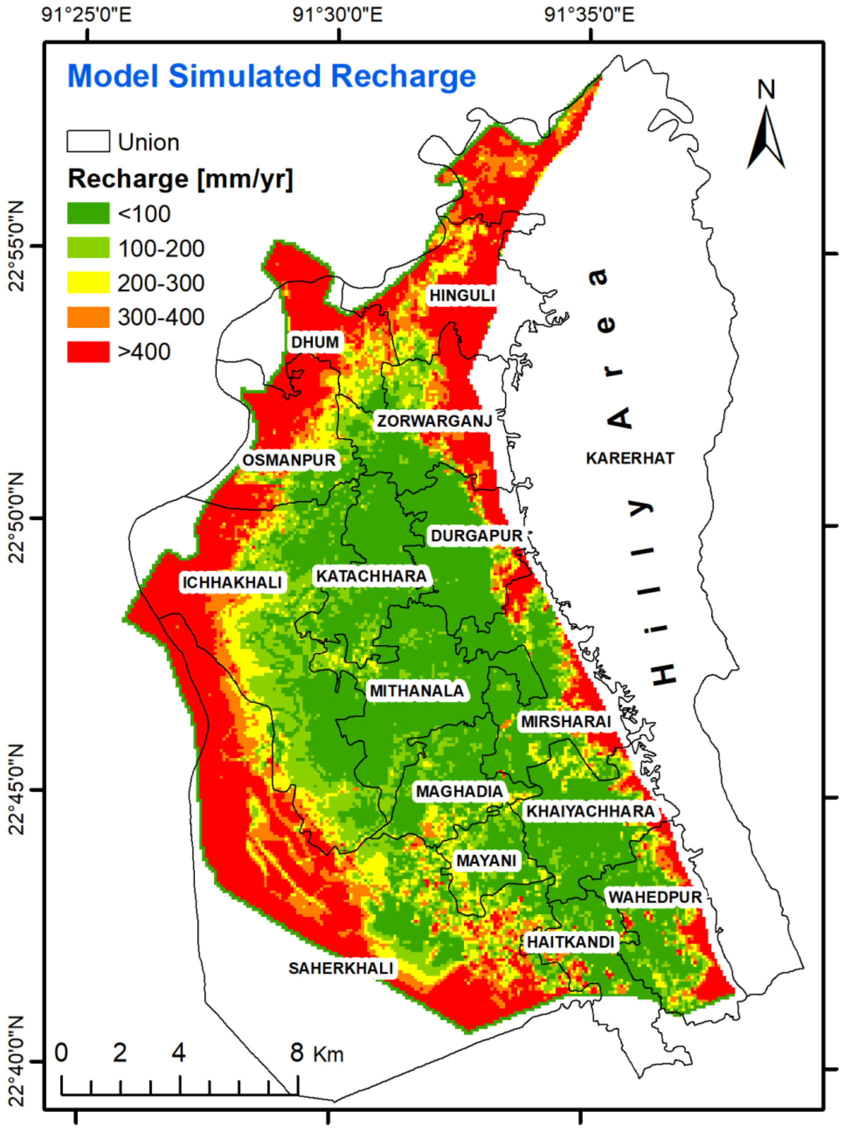

Figure 34: Model simulated recharge rate in the study area

3.2. Surface Water Resources and Flash Flood zoning and mitigation approach

This part is being processed and summarized and will be documented in the final report.

3.3. Model Simulation

The groundwater flow model was simulated in steady state to determine the current groundwater flow condition in the study area. Model simulated hydraulic head for all three aquifers (Figure 35) shows similar flow direction and generally shows the same trend as that based on the measured head data in the field.

The model now can be used in the analysis of various future water stress scenarios. Further simulation will be carried out to assess the sustainability of the groundwater in this area due to an increase of water demand in the future due to the planned development works.

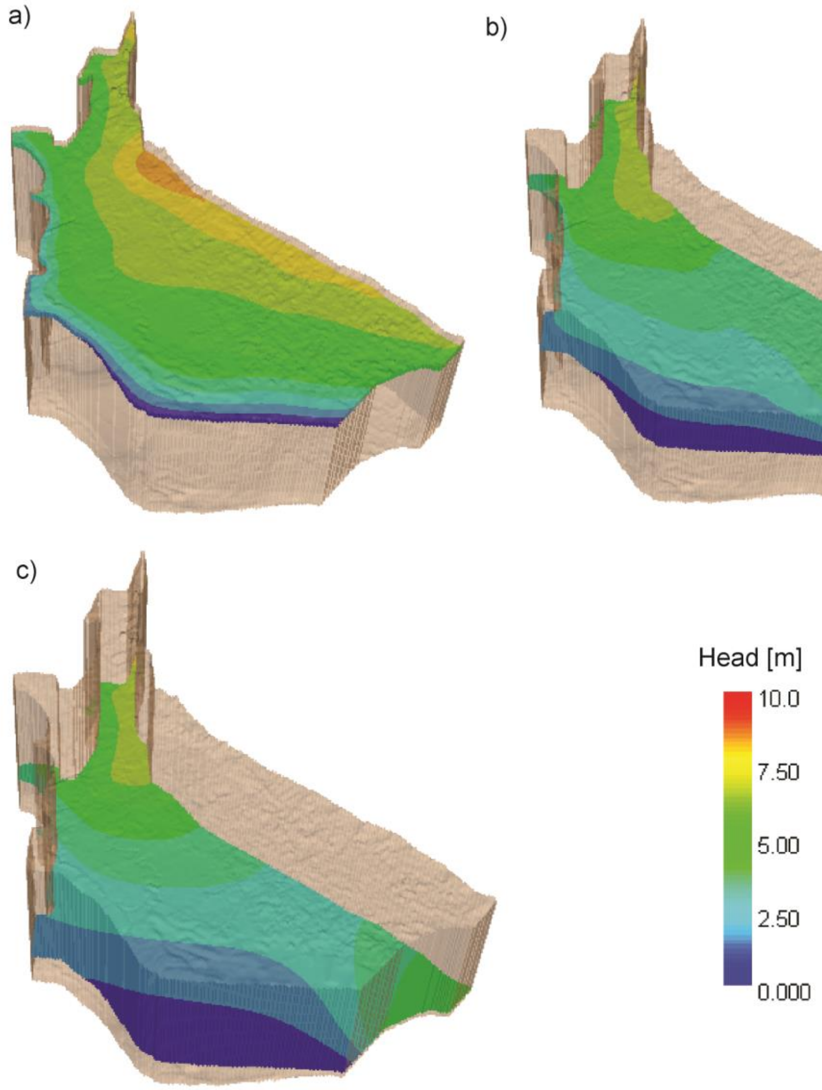

Figure 35: Model simulated hydraulic head for- a) Shallow aquifer, b) intermediate aquifer, and c) the deep aquifer

4. Discussion

This study comprises of extensive field work, laboratory analysis, and modeling to assess the availability and sustainability of the groundwater resources in Mirasharai Upazila. In this upazila both surface water and groundwater are available for use. Groundwater occurs primarily in three aquifers at various depth. However, the water quality of the shallow aquifer in a large part of the upazila in the south is not suitable for drinking purpose due to the presence of both arsenic and salinity. The remaining two aquifers that occurs on average below a depth of 70-100 m contains water suitable for drinking purpose. Both these deeper aquifers receives recharge in the northern part of the Upazila where all three aquifers are connected due to the lack of clay layers separating them. Presence of artesian condition in the northern part of the study area indicates that the recharge potential of the deep aquifer is very high. Development of the artesian aquifer in the north could be good option for drinking water supply throughout the Upazila, however, this need detail field and modeling investigation, which is not in the scope of the current study. Lack of clays and high recharge in the north also causes for some concern. Presence of water pollutants and contaminants in this area would be a potential threat for the groundwater to be contaminated. Care should be taken for carrying out any future development activities in the north that might discharge contaminated water on the surface and shallow subsurface.

Presence of high EC in the shallow aquifer only and not in the deep aquifer indicates that the Sandwip channel and the shallow aquifer is well connected and it does not have any connectivity with the deeper aquifers. However, the shallow salinity could also be due to inundation during storm surges in near past (100 years scale) or during the high sea level stand 5000 years before present, though, the parallel alignment of the EC contour and Sandwip channel suggest intrusion from the channel.

A groundwater flow model has been developed to assess the sustainability of the aquifers (deeper aquifers) to supply various projected high demand scenarios in near future. This part of the modeling is currently on going and would be finalized in about a month. The client is requested to share any plan for future development work in this area that they might have. It is to be noted that since the deeper aquifers contains fresh water all over the upazila without any exception and the shallow aquifer contain high arsenic and high salinity water, modeling focuses will be primarily on the two deeper aquifers.

There is one important concern about deep pumping in the southern part of the study area, where the aquitard between the shallow and the deep aquifer is thicker than 50 m. Heavy pumping from below that aquitard would cause a drop in pressure in the aquifer, and would initiate draining the overlying aquitard. The aquitard is composed of very soft marine clay. Upon drainage such clay layers have potential to lose more than 50% of its thickness causing subsidence. On the other hand, this thick aquitard can provide protection against downward migration of brackish water in the deep aquifer if the pumping in the deep aquifer in this part of the study area kept low. The current model can be used to predict the possibility of the migration of shallow high saline water to deep aquifer but it cannot be used to predict land subsidence. Land subsidence prediction requires more complex modelling which is not in the scope of this study.